

Article

Towards a Microscopic Theory of the Knight Shift in an Anisotropic, Multiband Type-II Superconductor

Richard A. Klemm 

Department of Physics, 4111 Libra Drive, University of Central Florida, Orlando, FL 32816-2385, USA; richard.klemm@ucf.edu; Tel.: 1-407-823-1543

Received: 24 November 2017; Accepted: 4 January 2018; Published: 29 January 2018

Abstract: A method is proposed to extend the zero-temperature Hall-Klemm microscopic theory of the Knight shift K in an anisotropic and correlated, multi-band metal to calculate $K(T)$ at finite temperatures T both above and into its superconducting state. The transverse part of the magnetic induction $\mathbf{B}(t) = \mathbf{B}_0 + \mathbf{B}_1(t)$ causes adiabatic changes suitable for treatment with the Keldysh contour formalism and analytic continuation onto the real axis. We propose that the Keldysh-modified version of the Gor'kov method can be used to evaluate $K(T)$ at high \mathbf{B}_0 both in the normal state, and by quantizing the conduction electrons or holes with Landau orbits arising from \mathbf{B}_0 , also in the entire superconducting regime for an anisotropic, multiband Type-II BCS superconductor. Although the details have not yet been calculated in detail, it appears that this approach could lead to the simple result $K_S(T) \approx a(\mathbf{B}_0) - b(\mathbf{B}_0)|\Delta(\mathbf{B}_0, T)|^2$, where $2|\Delta(\mathbf{B}_0, T)|$ is the effective superconducting gap. More generally, this approach can lead to analytic expressions for $K_S(T)$ for anisotropic, multiband Type-II superconductors of various orbital symmetries that could aid in the interpretation of experimental data on unconventional superconductors.

Keywords: Knight shift; Type-II superconductor; nuclear magnetic resonance; anisotropy; electron correlations

1. Introduction

In nuclear magnetic resonance (NMR) measurements of a nuclear spin, there is a difference between the resonance frequency of that spin when it is in a metal from when it is in vacuum or in an insulator. This is known as the Knight shift [1]. Although the temperature T dependence of the Knight shift in a superconductor $K_S(T)$ has long been considered to be a probe of the spin state of the paired electrons [2–4], the only theoretical basis for that assumption was the 1958 Yosida model that assumed the probed nuclear spins could be entirely neglected [5], and that the only quantity of interest was the T dependence of the zero-magnetic-field H limit of the electron spin susceptibility of an isotropic and uncorrelated Type-I superconductor [5]. This led for a BCS singlet-pair-spin superconductor to $K_S(T) \propto x/(1+x)$, where $x = (\beta/\Delta) \frac{d\Delta}{d\beta}$, $\beta = 1/T$, $\Delta(T)$ is one-half the BCS energy gap, and we set $k_B = 1$, so that $K_S(T) \rightarrow 0$ as $T \rightarrow 0$, unlike most experimental results [5].

For isotropic Type-I superconductors in the Meissner state, crushing the sample to a powder of crystallites the cross-sections of which were less than the magnetic penetration depth was usually found to provide a reasonable method for that conventional theory to be applicable [2–4]. In the first years following the BCS theory, a few elemental transition metal superconductors were found to behave somewhat differently, as $K_S(T)$ did not vanish as $T \rightarrow 0$ [6], and it was thought that surface impurity spin-orbit scattering could explain the near-cancellation of $K_S(0)$ in transition metals [6,7]. However, surface impurity spin-orbit scattering could not explain the observed non-vanishing $K_S(0)$ results observed in clean materials. It is now understood that there is also a component to the Knight shift due to the orbital motion of the electrons in a superconductor, and for an anisotropic superconductor, this orbital contribution to the Knight shift depends upon the magnetic induction B direction.

There have since been many examples of unexplained behaviors of the Knight shift in exotic superconductors. Since one possibility of a T -independent Knight shift result would be a parallel-spin, triplet pair-spin superconducting state, the use of the Knight shift has been considered to be a principal tool for the identification of a triplet pair-spin state. Some examples of triplet-pair-spin or some other types of exotic behavior claimed to exist in unusual materials based upon the unconventional Knight shift T -dependence are listed in the bibliography [8–14]. However, one of those materials was a quasi-one-dimensional organic superconductor [10,11], some examples of which often exhibit spin-density waves [15], and another was the very dirty sodium cobaltate hydrate material [12–14]. In the latter example, the upper critical field parallel to that layered compound is Pauli-limited, which normally only occurs when the magnetic field breaks the oppositely-oriented pair spins [16,17]. Since dirt drastically suppresses p -wave superconductivity [18], the sodium cobaltate hydrate Knight shift results, if correct, are likely to arise from some other mechanism.

Moreover, in highly anisotropic Type-II superconductors, such as the cuprates and heavy fermion materials, other significant breakdowns in the Yosida theory have been found to exist. In the first Knight shift measurements on the cuprate $\text{YBa}_2\text{Cu}_3\text{O}_{7-\delta}$, Bennett et al. found that the Yosida theory appeared to work for the ^{63}Cu spins in the CuO chains for all applied H directions, although the orbital contributions are different for each of those three orthogonal H directions, and it also appeared to work well for the ^{63}Cu spins in the CuO_2 planes when the strong constant H was applied parallel to the CuO_2 layers. However, when H was applied normal to the CuO_2 layers, no T dependence to the Knight shift was observed in that cuprate [19]. This result was later described by Slichter as possibly being due to a “fortuitous” cancelation of the effect from an isolated planar ^{63}Cu spin by its interaction with its near-neighbor planar ^{63}Cu spins [20]. Subsequently, in a number of layered correlated superconductors, the T dependence of the Knight shift probes of the nuclear spins in the layers with the field applied normal to the layers has been observed to vary strongly with field strength, approaching a constant $K_S(T)$ in the large normal field strength limit, as first observed by Bennett et al. [19–24].

Especially in the case of Sr_2RuO_4 , numerous Knight shift measurements of the ^{17}O , ^{99}Ru , ^{101}Ru , and ^{87}Sr have all led to temperature-independent Knight shift measurements [25–27], as did polarized neutron scattering experiments [28]. These experiments were all interpreted as evidence for a parallel-spin pair state in that material. However, several upper critical field measurements with the field parallel to the layers showed strong Pauli limiting effects [29,30], which is inconsistent with a parallel-spin pair state [31,32]. In addition, the fact that T -independent Knight shift measurements were obtained for the field both parallel and perpendicular to the RuO_2 layers is incompatible with any of the crystal point-group-compatible p -wave states. Thus, the only way for a T -independent Knight shift to legitimately arise from a parallel-pair-spin state in both field directions is for the d -vector (the vector describing the components of the three triplet spin states) to rotate with the magnetic field [33,34]. This argument was used to show that while the upper critical field of Sr_2RuO_4 is strongly Pauli limited for the field applied parallel to the layers, it could possibly be consistent with one or more p -wave helical states, provided that the d -vector is allowed to rotate freely with the magnetic field direction [32]. This means that spin-orbit coupling with the lattice would have to be negligible. However, there is strong evidence that spin-orbit coupling in Sr_2RuO_4 is very strong at some points on the Fermi surface, ruling out such d -vector rotation possibilities [35]. More worrisome for the Knight shift measurement results is the fact that carefully performed scanning tunneling measurements of the electronic density of states provided very strong evidence of a nodeless superconducting order parameter orbital symmetry in Sr_2RuO_4 [17,36], consistent with a nearly isotropic gap function that is essentially identical on all three of its Fermi surfaces. Since the theories behind the Pauli limiting effects and the BCS gap density of states are very well established, but the Knight shift measurement interpretations rely entirely on the complete neglect of the probed nuclear spins, the development of a microscopic theory of the T dependence of the Knight shift in anisotropic and correlated Type-II superconductors is sorely needed.

We further note that the time dependence of a spin-1/2 particle in a classic magnetic resonance experiment is now a textbook example of an exactly soluble first quantization quantum mechanics problem giving rise to a Berry phase [37,38]. In that case, the Berry, or geometric, phase is a combination of the resonance profile with the frequency of the oscillatory transverse applied magnetic field. In higher spin I systems, there are $2I$ combinations of those two quantities, giving rise to a multiplet of Berry phases, as discussed in the following. Note that the probed nuclear spins of Sr_2RuO_4 are either 5/2 or 9/2. Since nothing was known about the Berry phase in 1958, its possible implications for the interpretation of Knight shift measurements have been generally and perhaps completely ignored in the literature.

In fairness to the pioneering work of Yosida [5], there have been a few cases in which a complete lack of any T -dependence to the Knight shift has been confirmed by other experiments consistent with a parallel-pair-spin superconducting state [39–41]. These are for the uranium-based compounds UCoGe and UPt_3 , for which the T -independent Knight shift in UCoGe is in agreement with the general assessment of the upper critical field and muon depolarization experiments [18,40]. In UPt_3 , the seeming incompatibility of the Knight shift and the upper critical field appears to have been resolved by polarized neutron diffraction experiments [41], favoring a parallel-spin pair state in all three superconducting phases. In the ferromagnetic superconductors UGe_2 , UCoGe , and URhGe , the weak Ising-like ferromagnetism appears to allow for a parallel-spin, p -wave superconducting order parameter in the plane perpendicular to the ferromagnetism, but the Knight shift measurements have not yet been made on URhGe and UGe_2 , the latter of which is only superconducting under pressure. In these three ferromagnetic superconductors, there is at least a plausible mechanism for a parallel-spin pair superconducting state, and in URhGe the upper critical field fits the predictions for all three crystal axis directions of a parallel-spin p -wave polar state fixed to the crystal a -axis direction normal to the c -axis Ising ferromagnetic order [40,42], and there is a reentrant, high field phase that violates the Pauli limit by a factor of 20 [40]. In order to obtain further evidence that the classic Yosida interpretation of a T -independent $K_S(T)$ can correctly imply a parallel-spin superconducting state, we urge that ^{73}Ge , with a strong nuclear moment, (or possibly ^{103}Rh , with a much weaker nuclear moment) $K_S(T)$ measurements on URhGe be carefully performed in the low-field superconducting phase.

2. The Model

The first microscopic model of the Knight shift at $T = 0$ in anisotropic and correlated metals was recently presented by Hall and Klemm [43]. This model assumed that the applied magnetic fields probe the nuclear spins, and the spins of the electrons orbiting the nucleus interact with the nucleus via the hyperfine interaction in the form of a diagonal \mathbf{D} tensor with two distinct components $D_x = D_y \neq D_z$. The assumption $D_x = D_y$ was made to simplify the calculations, as discussed in more detail in the following. After interacting with the nuclear spins, the orbital electrons can be excited into one of multiple bands, each of which was assumed to have an ellipsoidal Fermi surface of arbitrary anisotropy and shape. The orbital motion of the electrons in each of these bands was constrained by the strong, time-independent part \mathbf{B}_0 of the magnetic induction $\mathbf{B}(t)$ to be in Landau levels, and the electron spins also could interact weakly with \mathbf{B}_0 . It was found that the self-energy due to D_z led to the Knight shift, and that due to $D_x = D_y$ led to the first formulas for the linewidth changes associated with the Knight shift at $T = 0$. However, since those calculations were made at $T = 0$, they could not be used to probe the superconducting state. In the following, a method is proposed to do so.

Following Haug and Jauho [44], we write the Hamiltonian as $\mathcal{H} = \mathcal{H}_0 + \mathcal{H}_{\text{int}} + \mathcal{H}'(t)$, where $\mathcal{H}_0 + \mathcal{H}_{\text{int}}$ is the time-independent part and $\mathcal{H}'(t)$ is the time-dependent part due to the oscillatory (or pulsed) magnetic field transverse to the constant applied magnetic field \mathbf{H}_0 , and the time-independent part consists of the simple (or exactly soluble) part \mathcal{H}_0 and the interaction part \mathcal{H}_{int} that involves the interactions between the particles that must be treated perturbatively. In the case at hand, there are four types of particles: (1) the nuclear spins probed in the NMR experiment, which are assumed to have the general spin $I \neq 0$ with $(2I + 1)$ substates denoted m_I ; (2) the local

orbital electrons surrounding each of the nuclei probed in the NMR experiment; (3) the conduction electrons or holes that propagate from the local nuclei throughout the metal/superconductor; and (4) the superconducting Cooper pairs of electrons or holes. We note that complicated materials such as Sr_2RuO_4 contain multiple Fermi surfaces, which can be a mix of electron and hole Fermi surfaces. In this model, we do not account for competing ferromagnetism or charge-density wave (CDW) or spin-density wave (SDW) formation, at least one of which is normally present in the transition metal dichalcogenides, the organic layered superconductors, the cuprates, the iron pnictides, and the ferromagnetic superconductors. Such competing effects will be the subjects of future studies.

2.1. The Simple Hamiltonian \mathcal{H}_0

Since in an NMR experiment, the applied magnetic field can be applied in any direction, we assume the resulting constant magnetic induction $\mathbf{B}_0 = B_0(\sin\theta \cos\phi, \sin\theta \sin\phi, \cos\theta) = B_0\hat{\mathbf{r}}$ with respect to the crystalline Cartesian x, y, z axes. We then quantize the spins along \mathbf{B}_0 . We thus write

$$\mathcal{H}_0 = \mathcal{H}_{n,0} + \mathcal{H}_{e,0} + \mathcal{H}_{\text{cond},0} \quad , \quad (1)$$

where

$$\mathcal{H}_{n,0} = -\omega_n \sum_{i,m_I} m_I a_{i,m_I}^\dagger a_{i,m_I} \quad , \quad (2)$$

$$\mathcal{H}_{e,0} = \sum_{i,q,\sigma} [\epsilon_q - \sigma\omega_e/2] b_{i,q,\sigma}^\dagger b_{i,q,\sigma} \quad , \quad (3)$$

$$\mathcal{H}_{\text{cond},0} = \sum_{j,\sigma} \int d^3\mathbf{r}_j \psi_{j,\sigma}^\dagger(\mathbf{r}_j) \left(\sum_{\nu=1}^3 \frac{1}{2m_{j,\nu}} [\nabla_{j,\nu}/i - eA_{j,\nu}(\mathbf{r}_j)]^2 - \sigma\omega'_{j,e}/2 \right) \psi_{j,\sigma}(\mathbf{r}_j) \quad , \quad (4)$$

where e is the electronic charge, a_{i,m_I}^\dagger creates a nucleus of spin I in the subspin state $m_I = -I, -I + 1, \dots, I - 1, I$ at the atomic position i , $b_{i,q,\sigma}^\dagger$ creates an electron with energy ϵ_q and spin-1/2 eigenstates indexed by $\sigma = \pm 1$ orbiting that nucleus at site i , where $q \in (n, \ell, m)$ is nominally its weak-spin-orbit local electron orbital quantum number set [or its fully relativistic set (n, j)], $\psi_{j,\sigma}^\dagger(\mathbf{r}_j)$ creates an electron or hole with spin eigenstate $\sigma = \pm 1$ at position \mathbf{r}_j in the j^{th} conduction band, $\omega_n = \boldsymbol{\mu}_n \cdot \mathbf{B}_0$, $\omega_e = \boldsymbol{\mu}_e \cdot \mathbf{B}_0$, $\omega'_{j,e} = \boldsymbol{\mu}_e \cdot \mathbf{g}_j \cdot \mathbf{B}_0$ are respectively the Zeeman energies for the probed nucleus, local orbital electrons, and conduction electrons, respectively, $\boldsymbol{\mu}_n$ is the nuclear magneton for the probed nucleus (the value of which can be positive or negative), $|\boldsymbol{\mu}_e| = \mu_B$ is the Bohr magneton, $\mathbf{g}_j \cdot \mathbf{B}_0$ defines the quantization axis direction for the anisotropic but assumed diagonal \mathbf{g}_j tensor in the j^{th} of the N_b conduction bands with effective mass $m_{j,\nu}$ in the ν^{th} spatial direction, $A_{j,\nu}(\mathbf{r}_j)$ is the ν^{th} component of the magnetic vector potential at the position \mathbf{r}_j of the conduction electron in the j^{th} band, $\mathbf{B}_0 = \nabla_{j,\nu} \times A_{j,\nu}$ is the magnetic induction that is independent of j, ν , and the time t , $i = \sqrt{-1}$, and we set $\hbar = 1$. Here we use the previous notation [43], but rearrange the terms in the overall Hamiltonian in order to properly take account of both the t and T dependencies essential for probing the superconducting state. We note that for integer or half-integer I , the nuclei would normally be expected to obey Bose-Einstein or Fermi-Dirac statistics, but since different nuclei correspond to different atoms and do not come in contact with one another, that statistics is not expected to be an important feature of the Knight shift. Equation (1) is the extension to arbitrary nuclear spin I of the bare Hamiltonian studied previously, except that $\mathcal{H}_{\text{cond},0}$ was the time independent part of $H_{A,2}$ [43]. We note that for a diagonal \mathbf{g}_j tensor,

$$\omega'_{j,e} = \mu_B B_0 [g_{j,xx} \sin^2\theta \cos^2\phi + g_{j,yy} \sin^2\theta \sin^2\phi + g_{j,zz} \cos^2\theta]^{1/2}. \quad (5)$$

As a starting point, we assume \mathbf{B}_0 is uniform in the probed material, but when the material goes into the superconducting state, and \mathbf{B}_0 is in an arbitrary direction with respect to the crystal axes, this is only true at the upper critical field H_{c2} above which the superconductor becomes a normal

metal [17,45]. However, in the mixed state for which the time-independent part of the applied magnetic field \mathbf{H}_0 satisfies $\mathbf{H}_{c1} < \mathbf{H}_0 < \mathbf{H}_{c2}$, if \mathbf{H}_0 is along a crystal axis, the direction of \mathbf{B}_0 is the same as the direction of \mathbf{H}_0 [17,46].

2.2. The Time-Independent Interaction Hamiltonian \mathcal{H}_{int}

We write the time-independent interaction part \mathcal{H}_i of the Hamiltonian as

$$\mathcal{H}_{\text{int}} = \mathcal{H}_{hf} + \mathcal{H}_{e,\text{int}} + \mathcal{H}_{e,\text{cond}} + \mathcal{H}_{\text{sc}} \quad , \quad (6)$$

where

$$\mathcal{H}_{hf} = -\frac{D_z}{4} \sum_{i,q,\sigma,m_I} m_I \sigma a_{i,m_I}^\dagger a_{i,m_I} b_{i,q,\sigma}^\dagger b_{i,q,\sigma} - \frac{D_x}{2} \sum_{i,q,\sigma,m_I} A_{I,m_I}^\sigma a_{i,m_I+\sigma}^\dagger a_{i,m_I} b_{i,q,-\sigma}^\dagger b_{i,q,\sigma} \quad , \quad (7)$$

$$\mathcal{H}_{e,\text{int}} = \frac{1}{2} \sum_{i,q,\sigma} U_q \hat{n}_{i,q,\sigma} \hat{n}_{i,q,-\sigma} = \sum_{i,q} U_q b_{i,q,\uparrow}^\dagger b_{i,q,\uparrow} b_{i,q,\downarrow}^\dagger b_{i,q,\downarrow} \quad (8)$$

$$\mathcal{H}_{e,\text{cond}} = \sum_{i,q,j,\sigma} \int d^3 \mathbf{r}_j \left(v_{i,q,j} \psi_{j,\sigma}^\dagger(\mathbf{r}_j) b_{i,q,\sigma} + H.c. \right) \delta^{(3)}(\mathbf{r}_j - \mathbf{r}_i) \quad , \quad (9)$$

where $A_{I,m_I}^\sigma = \sqrt{I(I+1) - m_I(m_I + \sigma)}$, and depending upon what is calculated, the superconducting pairing interaction may be written either in real space as

$$\mathcal{H}_{\text{sc}}^{\text{pos}} = \frac{1}{2} \sum_{j,j',\sigma,\sigma'} \int d^3 \mathbf{r}_j \int d^3 \mathbf{r}'_{j'} \psi_{j,\sigma}^\dagger(\mathbf{r}_j) \psi_{j',\sigma'}^\dagger(\mathbf{r}'_{j'}) V_{j,j';\sigma,\sigma'}(\mathbf{r}_j - \mathbf{r}'_{j'}) \psi_{j',\sigma'}(\mathbf{r}'_{j'}) \psi_{j,\sigma}(\mathbf{r}_j) \quad , \quad (10)$$

or in momentum space as

$$\mathcal{H}_{\text{sc}}^{\text{mom}} = \frac{1}{2} \sum_{j,j',\sigma,\sigma'} \int \frac{d^3 \mathbf{k}_j}{(2\pi)^3} \int \frac{d^3 \mathbf{k}'_{j'}}{(2\pi)^3} \psi_{j,\sigma}^\dagger(\mathbf{k}_j) \psi_{j',\sigma'}^\dagger(\mathbf{k}'_{j'}) V_{j,j';\sigma,\sigma'}(\mathbf{k}_j - \mathbf{k}'_{j'}) \psi_{j',\sigma'}(\mathbf{k}'_{j'}) \psi_{j,\sigma}(\mathbf{k}_j) \quad . \quad (11)$$

Although it appears at first sight to be easier to extend the calculation of the Knight shift into the BCS superconducting state by using $\mathcal{H}_{\text{sc}}^{\text{pos}}$ in order to include the Zeeman terms, we have included the momentum-space pairing interaction $\mathcal{H}_{\text{sc}}^{\text{mom}}$ for *p*-wave superconductors in magnetic fields [18,42], for which the simplest single-band parallel-spin pairing interaction $V_{j,j';\sigma,\sigma'}(\mathbf{k}_j - \mathbf{k}'_{j'}) = -V_0 \delta_{j,j'} \delta_{\sigma,\sigma'} \mathbf{k}_1 \cdot \mathbf{k}'_1$ [18], and a modification of $\mathcal{H}_{\text{sc}}^{\text{mom}}$ more naturally treats the pairing of conduction electrons (or holes) in the presence of a strong \mathbf{B}_0 .

We note that $\sigma = \pm 1$ present in A_{I,m_I}^σ corresponds to the correct matrix elements for raising and lowering the m_I value and also corresponds to our description of the spin-1/2 electron spins [43]. Of course, m_I and σ are restricted by $-I \leq m_I, m_I + \sigma \leq I$. The first three of these terms were presented previously [43], except for a slightly different normalization factor proportional to N_b , and respectively represent the hyperfine interaction between the nuclear and surrounding orbital electrons, the effective local electron correlation interaction, and the effective Anderson interaction that allows an orbital electron to leave a local atomic site and jump into a conduction band [47]. The last term \mathcal{H}_{sc} is responsible for superconducting pairing, and in the form presented allows for pairing between electrons or holes in different bands and with either the same ($\sigma' = \sigma$) or different ($\sigma' = -\sigma$) spins. In most superconductors, interband pairing is generally considered to be less important than is intraband pairing, but such complications might be important in cases such as Sr_2RuO_4 , for which two of the bands are nearly identical. For standard BCS pairing, we would have $V_{\sigma,\sigma'}(\mathbf{r}_j - \mathbf{r}'_{j'}) \rightarrow -V_0 \delta_{\sigma',-\sigma} \delta_{j,j'} \delta^{(3)}(\mathbf{r}_j - \mathbf{r}'_{j'})$, at least in the standard approximation. For parallel-spin *p*-wave superconductors, one cannot assume the paired electrons are at the same location, but different approximations have been found to give reliable results for the upper critical induction in ferromagnetic superconductors [18,32,42,48,49].

2.3. The Time-Dependent Hamiltonian $\mathcal{H}'(t)$

The crucial part of a magnetic resonance experiment arises from the time-dependent field transverse to the stronger constant magnetic field. In a conventional NMR experiment, the time-dependent induction $\mathbf{B}_1(t)$ oscillates in the plane normal to the strong, constant magnetic induction \mathbf{B}_0 . For $\mathbf{B}_0 = B_0(\sin\theta \cos\phi, \sin\theta \sin\phi, \cos\theta) = B_0\hat{\mathbf{r}}$, one may then write $\mathbf{B}_1(t) = B_1\{\cos[\omega_0(t-t_0)]\hat{\boldsymbol{\theta}} - \sin[\omega_0(t-t_0)]\hat{\boldsymbol{\phi}}\}$, where $\hat{\boldsymbol{\theta}} = (\cos\theta \cos\phi, \cos\theta \sin\phi, -\sin\theta)$ and $\hat{\boldsymbol{\phi}} = (-\sin\phi, \cos\phi, 0)$ in the same Cartesian coordinates, and in order not to get confused with the time contours, we may choose $\mathbf{B}_1(t_0)$ to be along $\hat{\boldsymbol{\theta}}$. This is the classic way to obtain a resonance in the power spectrum associated with flipping an electron or proton spin from up to down, or in a spin I nucleus, to obtain a regular pattern of resonance frequencies associated with changes in the multiple Zeeman-like nuclear spin levels. Since one generally takes $B_1 \ll B_0$, this classic case is generally adiabatic [37,38], and is the simplest case to treat analytically.

For the above classic NMR case of a single angular frequency ω_0 in $\mathbf{B}_1(t)$, we then have

$$\mathcal{H}'(t) = \mathcal{H}'_n(t) + \mathcal{H}'_e(t) + \mathcal{H}'_{\text{cond}}(t) \quad , \quad (12)$$

$$\mathcal{H}'_n(t) = -\frac{\Omega_n}{2} \sum_{i,m_1,\sigma} e^{i\sigma\omega_0(t-t_0)} A_{I,m_1}^\sigma a_{i,m_1+\sigma}^\dagger a_{i,m_1} \quad , \quad (13)$$

$$\mathcal{H}'_e(t) = -\frac{\Omega_e}{2} \sum_{i,\sigma} e^{i\sigma\omega_0(t-t_0)} b_{i,\sigma}^\dagger b_{i,-\sigma} \quad , \quad (14)$$

$$\mathcal{H}'_{\text{cond}}(t) = -\frac{1}{2} \sum_{j,\sigma} e^{i\sigma\omega_0(t-t_0)} \int d^3\mathbf{r}_j \psi_{j,\sigma}^\dagger(\mathbf{r}_j) \Omega'_{j,e} \psi_{j,-\sigma}(\mathbf{r}_j) \quad , \quad (15)$$

where $\Omega_n = \mu_n B_1$, $\Omega_e = \mu_e B_1$, and $\Omega'_{j,e} = \boldsymbol{\mu}_e \cdot \mathbf{g}_j \cdot \mathbf{B}_1$, and A_{I,m_1}^σ is given by Equation (11) [43].

3. The Keldysh Contours

Following Haug and Jauho [44] and with regard to the contours, Rammer and Smith [50], we may treat the time and temperature dependence of the particles together in the same formulas, as long as we properly order the time integrations around the appropriate contours. When there is only one type of particle, which we take to be a fermion, the fields at the three-dimensional positions \mathbf{r}_1 and \mathbf{r}_1' evolve in time according to the simple Hamiltonian H_0 ,

$$\psi_{\mathcal{H}_0}(\mathbf{r}_1, t_1) \equiv \psi_{\mathcal{H}_0}(1) = e^{i\mathcal{H}_0 t_1} \psi(\mathbf{r}_1) e^{-i\mathcal{H}_0 t_1} \quad , \quad (16)$$

$$\psi_{\mathcal{H}_0}^\dagger(\mathbf{r}_1', t_1') \equiv \psi_{\mathcal{H}_0}^\dagger(1') = e^{i\mathcal{H}_0 t_1'} \psi^\dagger(\mathbf{r}_1') e^{-i\mathcal{H}_0 t_1'} \quad , \quad (17)$$

with its density matrix also involving only \mathcal{H}_0 (and the number operator $\hat{\mathcal{N}}$ in the grand canonical ensemble statistics),

$$\hat{\rho}_0 = \frac{e^{-\beta(\mathcal{H}_0 - \mu\hat{\mathcal{N}})}}{\text{Tr}[e^{-\beta(\mathcal{H}_0 - \mu\hat{\mathcal{N}})}]} \quad (18)$$

and the Green function is given by the two contour integration paths C and C_{int} sketched in Figure 1,

$$G(1, 1') = -i \frac{\text{Tr}\left\{\hat{\rho}_0 T_C[\mathcal{S}_{C_{\text{int}}}' \mathcal{S}_C' \psi_{\mathcal{H}_0}(1) \psi_{\mathcal{H}_0}^\dagger(1')]\right\}}{\text{Tr}[T_C(\mathcal{S}_{C_{\text{int}}}' \mathcal{S}_C')]} \quad , \quad (19)$$

$$\mathcal{S}'_C = \exp\left[-i \int_C d\tau \mathcal{H}'_{\mathcal{H}_0}(\tau)\right] \quad , \quad (20)$$

$$\mathcal{S}'_{C_{\text{int}}} = \exp\left[-i \int_{C_{\text{int}}} d\tau \mathcal{H}_{\text{int}, \mathcal{H}_0}(\tau)\right] \quad , \quad (21)$$

where the operators in $\mathcal{H}'_{\mathcal{H}_0}(\tau)$ and $\mathcal{H}_{\text{int},\mathcal{H}_0}(\tau)$ evolve in time via the easily soluble Hamiltonian \mathcal{H}_0 . The Greek letter τ implies that one needs to consider it as being just above or just below the real axis until the contours merge into one. Roman lettering (t) indicates the integrals are on the real axis.

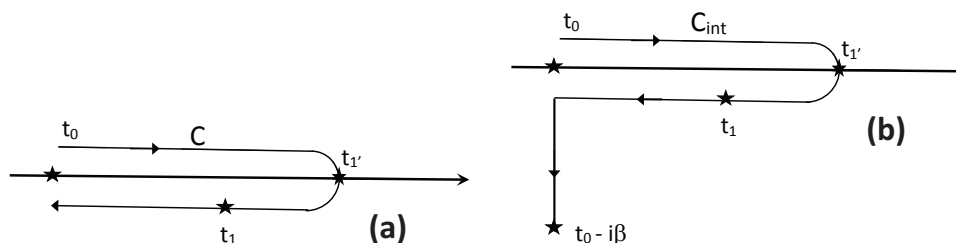


Figure 1. (a) Sketch of the “closed path” contour C ; (b) Sketch of the “interaction” contour C_{int} .

For the case of the time-dependent Hamiltonian $\mathcal{H}'(t)$ making adiabatic changes, as in the case considered here, the two contours C and C_{int} respectively shown in Figure 1a,b merge into contour C shown in Figure 1a. We use the standard short-hand notation

$$G(1,1') = -i\langle T_C[\psi_{\mathcal{H}}(1)\psi_{\mathcal{H}}^\dagger(1')] \rangle, \quad (22)$$

where the particle type, its position, and its energy are still undefined. In order to treat the various time orderings on the contour C , we define the following in the Heisenberg representation for the full Hamiltonian \mathcal{H} ,

$$G^>(1,1') = -i\langle \psi_{\mathcal{H}}(1)\psi_{\mathcal{H}}^\dagger(1') \rangle, \quad (23)$$

$$G^<(1,1') = +i\langle \psi_{\mathcal{H}}^\dagger(1')\psi_{\mathcal{H}}(1) \rangle, \quad (24)$$

$$G^C(1,1') = -i\langle T[\psi_{\mathcal{H}}(1)\psi_{\mathcal{H}}^\dagger(1')] \rangle = \Theta(t_1 - t_1')G^>(1,1') + \Theta(t_1' - t_1)G^<(1,1'), \quad (25)$$

$$G^{\tilde{C}}(1,1') = -i\langle \tilde{T}[\psi_{\mathcal{H}}(1)\psi_{\mathcal{H}}^\dagger(1')] \rangle = \Theta(t_1 - t_1')G^<(1,1') + \Theta(t_1' - t_1)G^>(1,1'), \quad (26)$$

where the ordinary time-ordering operator T and inverse-time-ordering operator \tilde{T} describe opposite directions in time, as sketched by lines C_1 and C_2 in Figure 2. We note that $G^C(1,1') + G^{\tilde{C}}(1,1) = G^<(1,1') + G^>(1,1')$, so only three of these Green functions are linearly independent.

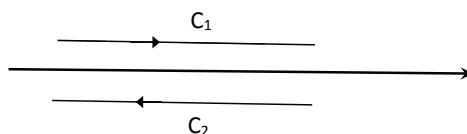


Figure 2. Sketch of the Keldysh contour C_K .

Here we need to describe three particles, all of which are effectively fermions.

3.1. Bare Nuclear Contour Green Functions

We first consider the nuclei, which are assumed not to interact with one another, as they are fixed in the crystalline locations, which if there is more than one isotope of a particular type with spin I , may be at a random selection of crystalline sites. In the presence of the constant magnetic induction B_0 , it can be in any one of the $2I + 1$ manifold of nuclear Zeeman states, but because each of these local states at the probed nuclear site i can be either unoccupied or singly occupied, this manifold of local

nuclear spin states is precisely that of a fermion with $(2I + 1)$ states. Its occupancy in the local state m_I on site i in the grand canonical ensemble is therefore easily seen to be

$$\langle \hat{n}_{i,m_I}^n \rangle = \frac{1}{e^{\beta(\epsilon_{m_I} - \mu_{\text{ncp}})} + 1}, \quad (27)$$

where $\epsilon_{m_I} = -\omega_n m_I$ and μ_{ncp} is the nuclear chemical potential. We then have for the bare nuclear Green functions with $\mathcal{H} = \mathcal{H}_{0,n}$,

$$G_{i,i';m_I,m_I'}^{(0,n),<}(1,1') = +i\delta_{i,i'}\delta_{m_I,m_I'}e^{i\epsilon_{m_I}(t_1-t_{1'})}\langle \hat{n}_{i,m_I}^n \rangle, \quad (28)$$

$$G_{i,i';m_I,m_I'}^{(0,n),>}(1,1') = -i\delta_{i,i'}\delta_{m_I,m_I'}e^{i\epsilon_{m_I}(t_1-t_{1'})}[1 - \langle \hat{n}_{i,m_I}^n \rangle], \quad (29)$$

and $G_{i,i';m_I,m_I'}^{(0,n),C}(1,1')$, $G_{i,i';m_I,m_I'}^{(0,n),\tilde{C}}(1,1')$ are constructed from these according to Equations (25) and (26). There are only three distinct bare neutron Green functions. This is also true when interactions are included [44]. Although it is somewhat surprising that the nuclear occupation density has the Fermi function form even for integral spin I , this is due to the nuclear Zeeman magnetic level occupancy being either 0 or 1 for each level on a given probed nuclear site.

3.2. Bare Orbital Electron Contour Green Functions

For the surrounding orbital electrons, we assume that the magnetic induction $\mathbf{B}_0 + \mathbf{B}_1(t)$ is sufficiently weak that it does not change the electronic structure of the orbital electrons or lead to transitions between the orbital electron states and energy levels. Thus, we assume that it only interacts with the orbital electron spins. We note that this is expected to be a good approximation, as the total charge of the nucleus plus its orbital electrons is on the order of one electron charge (for an ion), and the mass of the ion is so large that any Landau levels describing the orbital electrons and their central nucleus is completely negligible in comparison with the Landau levels of the conduction electrons. The only point then to consider for the interaction of \mathbf{B}_0 with the orbital electrons is that there can be either 0, 1, or 2 electrons in a given orbital energy ϵ_q , and two possible magnetic energies for up and down spins. Hence, it is elementary to show that the average orbital electron occupation number in the grand canonical ensemble is

$$\langle \hat{n}_{i,q,\sigma}^e \rangle = \frac{1}{e^{\beta(\epsilon_q - \sigma\omega_e/2 - \mu_{\text{ecp}})} + 1}, \quad (30)$$

where μ_{ecp} is the orbital electron chemical potential. It is then easy to show that the bare orbital electron Green functions are

$$G_{i,i';q,q'}^{(0,e),<}(1,1') = +i\delta_{i,i'}\delta_{q,q'}\delta_{\sigma,\sigma'}e^{i(\epsilon_q - \sigma\omega_e/2)(t_1-t_{1'})}\langle \hat{n}_{i,q,\sigma}^e \rangle, \quad (31)$$

$$G_{i,i';q,q'}^{(0,e),>}(1,1') = -i\delta_{i,i'}\delta_{q,q'}\delta_{\sigma,\sigma'}e^{i(\epsilon_q - \sigma\omega_e/2)(t_1-t_{1'})}[1 - \langle \hat{n}_{i,q,\sigma}^e \rangle], \quad (32)$$

and the time-ordered and inverse-time-ordered bare orbital electron Green functions are obtained analogously using Equations (25) and (26). Only three of the bare orbital electron Green functions are linearly independent. This is also true when interactions are included [44].

3.3. Bare Conduction Electron Contour Green Functions

In a normal metal (above the superconducting transition of all superconductors including the cuprates and the record high transition temperature superconductor hydrogen sulfide, which probably transforms to H_3S under the 155 GPa pressure that causes it to become superconducting at 203 K [51]), the conduction electrons or holes propagate throughout the metal with wave vectors on or nearly

on one or more Fermi surfaces. Both the spins and the charges of the conduction electrons interact with B_0 , the spins via the Zeeman interaction and the charges couple to the magnetic vector potential, leading to Landau orbits. Here we assume each of these potentially multiple Fermi surfaces has an ellipsoidal shape, but the shapes and orientations of each of the Fermi surfaces can be different from one another.

We first use the Klemm-Clem transformations to transform each of the ellipsoidal conduction electron band dispersions into spherical forms [43,45]. For each ellipsoidal band, the anisotropic scale transformation that preserves the Maxwell equation $\nabla \cdot B_0 = 0$ transforms the elliptical Fermi surface into a spherical one, but rotates the transformed induction differently in each band. Then, one rotates these bands so that the rotated induction is along the z direction in each band [43]. In the j th band, the conduction electrons behave as free particles with wave vector $k_{j,\parallel}$ along the transformed \hat{z} direction, but propagate in Landau orbits indexed by the harmonic oscillator quantum number n_j . Thus, we need to quantize the conduction electron fields as $\tilde{\psi}_{j,n_j,\sigma}(k_{j,\parallel})$.

We therefore rewrite the transformed $\tilde{\mathcal{H}}_{\text{cond},0}$ as

$$\tilde{\mathcal{H}}_{\text{cond},0} = \sum_{j,\sigma} g_{L,j} \sum_{n_j=0}^{\infty} \int \frac{dk_{j,\parallel}}{2\pi} \tilde{\psi}_{j,n_j,\sigma}^\dagger(k_{j,\parallel}) [\varepsilon_j(n_j, k_{j,\parallel}) - \sigma \tilde{\omega}'_{j,e}/2] \tilde{\psi}_{j,n_j,\sigma}(k_{j,\parallel}), \quad (33)$$

$$\varepsilon_j(n_j, \tilde{k}_{j,\parallel}) = \frac{\tilde{k}_{j,\parallel}^2}{2m_j \alpha_j^2} + \frac{(n_j + 1/2)eB_0 \alpha_j}{m_j}, \quad (34)$$

$$\tilde{\omega}'_{j,e} = \mu_B B_0 \beta_j(\theta, \phi), \quad (35)$$

where $n_j = 0, 1, 2, \dots$ are the two-dimensional simple harmonic oscillator quantum numbers of the Landau orbits for band j , $k_{j,\parallel}$ are the free-particle dispersions along the transformed induction direction,

$$\alpha_j(\theta, \phi) = [\bar{m}_{j,1} \sin^2 \theta \cos^2 \phi + \bar{m}_{j,2} \sin^2 \theta \sin^2 \phi + \bar{m}_{j,3} \cos^2 \theta]^{1/2}, \quad (36)$$

$$m_j = (m_{j,1} m_{j,2} m_{j,3})^{1/3}, \quad (37)$$

$$\bar{m}_{j,\nu} = \frac{m_{j,\nu}}{m_j}, \quad (38)$$

$$\beta_j(\theta, \phi) = [g_{j,xx}^2 \bar{m}_{j,1} \sin^2 \theta \cos^2 \phi + g_{j,yy}^2 \bar{m}_{j,2} \sin^2 \theta \sin^2 \phi + g_{j,zz}^2 \bar{m}_{j,3} \cos^2 \theta]^{1/2}, \quad (39)$$

for a diagonal g_j tensor describing the spins of the j th conduction band, and

$$g_{L,j} = \frac{eB_0 \alpha_j}{2\pi} \quad (40)$$

is the spatially-transformed Landau degeneracy for a single electron in the j th band. We may then write the conduction electron occupation number as

$$\langle \hat{n}_{j,\tilde{k}_{j,\parallel},n_j,\sigma}^{\text{cond}} \rangle = \frac{1}{e^{\beta[\varepsilon_j(n_j, \tilde{k}_{j,\parallel}) - \sigma \tilde{\omega}'_{j,e}/2 - \mu_{\text{cond,cp}}]} + 1}, \quad (41)$$

where $\mu_{\text{cond,cp}}$ is the chemical potential of the conduction electrons. We note that all of the bands that cross this conduction electron chemical potential make important contributions to the Knight shift.

The bare conduction electron Green functions can then be found to be

$$G_{\substack{j,j',\bar{k}_{j,\parallel},\bar{k}'_{j',\parallel}; \\ n_j,n'_j,\sigma,\sigma'}}^{(0,\text{cond}),<}(1,1') = +i\delta_{j,j'}\delta_{\bar{k}_{j,\parallel},\bar{k}'_{j',\parallel}}\delta_{n_j,n'_j}\delta_{\sigma,\sigma'}g_{L,j}e^{i[\varepsilon_j(\bar{k}_{j,\parallel},n_j)-\sigma\tilde{\omega}'_e/2](t_1-t_1')}\langle\hat{n}_{i,\bar{k}_{j,\parallel},n_j,\sigma}^{\text{cond}}\rangle, \quad (42)$$

$$G_{\substack{j,j',\bar{k}_{j,\parallel},\bar{k}'_{j',\parallel}; \\ n_j,n'_j,\sigma,\sigma'}}^{(0,\text{cond}),>}(1,1') = -i\delta_{j,j'}\delta_{\bar{k}_{j,\parallel},\bar{k}'_{j',\parallel}}\delta_{n_j,n'_j}\delta_{\sigma,\sigma'}g_{L,j}e^{i[\varepsilon_j(\bar{k}_{j,\parallel},n_j)-\sigma\tilde{\omega}'_e/2](t_1-t_1')}[1-\langle\hat{n}_{i,\bar{k}_{j,\parallel},n_j,\sigma}^{\text{cond}}\rangle], \quad (43)$$

and the contour-ordered and inverse-contour-ordered bare conduction electron Green functions are obtained as in Equations (25) and (26), so that there are only three independent bare conduction electron Green functions.

Furthermore, due to the strong B_0 , we also need to spatially transform all of the other terms in the Hamiltonian that contain the conduction electrons. Thus, we have [43]

$$\tilde{\mathcal{H}}'_{\text{cond}}(t) = -\frac{1}{2}\sum_{j,\sigma}g_{L,j}e^{i\sigma\omega_0(t-t_0)}\sum_{n_j=0}^{\infty}\int\frac{dk_{j,\parallel}}{2\pi}\tilde{\psi}_{j,n_j,\sigma}^\dagger(k_{j,\parallel})\tilde{\Omega}'_{j,e}\tilde{\psi}_{j,n_j,-\sigma}(k_{j,\parallel}), \quad (44)$$

$$\tilde{\Omega}'_{j,e} \approx \mu_B B_1 \gamma_j(\theta, \phi), \quad (45)$$

$$\begin{aligned} \gamma_j(\theta, \phi) &= [g_{j,xx}^2(\bar{m}_{j,2} \sin^2 \theta \sin^2 \phi + \bar{m}_{j,3} \cos^2 \theta) \\ &\quad + g_{j,yy}^2(\bar{m}_{j,1} \sin^2 \theta \cos^2 \phi + \bar{m}_{j,3} \cos^2 \theta) + g_{j,zz}^2(\bar{m}_{j,1} \cos^2 \phi + \bar{m}_{j,2} \sin^2 \phi)]^{1/2}. \end{aligned} \quad (46)$$

4. Transformations in Time of the Operators with the Bare Hamiltonian

In order to proceed with the perturbation expansions, we first need to transform the nuclear, orbital electronic, and conduction electronic operators in real time, using the bare Hamiltonian in Equation (1). For the nuclear and orbital electronic operators, this is elementary. We have

$$\begin{aligned} a_{i,m_I}(t) &= e^{i\mathcal{H}_{n,0}t}a_{i,m_I}e^{-i\mathcal{H}_{n,0}t} \\ \frac{da_{i,m_I}(t)}{dt} &= i[\mathcal{H}_{n,0}, a_{i,m_I}(t)] \\ &= +i\omega_n m_I a_{i,m_I}(t), \end{aligned} \quad (47)$$

and integrating the elementary differential equation, we immediately find

$$a_{i,m_I}(t) = e^{i\omega_n m_I t}a_{i,m_I}(0) = e^{i\omega_n m_I (t-t_0)}a_{i,m_I}(t_0), \quad (48)$$

in order to use this in Equation (16). The quantity $a_{i,m_I+\sigma}^\dagger(t)$ is instantly obtained from the Hermitian conjugate of Equation (52) and letting $m_I \rightarrow m_I + \sigma$, and hence $a_{i,m_I+\sigma}^\dagger(t) = e^{-i\omega_n(m_I+\sigma)(t-t_0)}a_{i,m_I+\sigma}^\dagger(t_0)$, so that the time-transformed Equation (16) becomes

$$\mathcal{H}'_{n,\mathcal{H}_{n,0}}(t) = -\frac{\Omega_n}{2}\sum_{i,m_I,\sigma}e^{i\sigma(\omega_0-\omega_n)(t-t_0)}A_{I,m_I}^\sigma a_{i,m_I,\sigma}^\dagger(t_0)a_{i,m_I}(t_0). \quad (49)$$

Similarly, for the local orbital electron operators, we have

$$b_{i,q,\sigma}(t) = e^{i\mathcal{H}_{e,0}(t-t_0)}b_{i,q,\sigma}(t_0)e^{-i\mathcal{H}_{e,0}(t-t_0)} \quad (50)$$

$$= e^{-i(\varepsilon_q-\sigma\omega_e/2)(t-t_0)}b_{i,q,\sigma}(t_0), \quad (51)$$

and

$$\mathcal{H}'_{e,\mathcal{H}_{e,0}}(t) = -\frac{\Omega_e}{2}\sum_{i,q,\sigma}e^{i\sigma(\omega_0-\omega_e)(t-t_0)}b_{i,q,\sigma}^\dagger(t_0)b_{i,q,-\sigma}(t_0), \quad (52)$$

For the spatially-transformed conduction electron operators,

$$\tilde{\psi}_{j,n_j,\sigma}(k_{j,\parallel}, t) = e^{i\tilde{\mathcal{H}}_{\text{cond},0}(t-t_0)} \tilde{\psi}_{j,n_j,\sigma}(k_{j,\parallel}, t_0) e^{-i\tilde{\mathcal{H}}_{\text{cond},0}(t-t_0)} \quad (53)$$

$$= e^{-i[\varepsilon_j(n_j, k_{j,\parallel}) - \sigma\tilde{\omega}'_{j,e}/2](t-t_0)} \tilde{\psi}_{j,n_j,\sigma}(k_{j,\parallel}, t_0), \quad (54)$$

so that the time-transformed Equation (44). becomes

$$\tilde{\mathcal{H}}'_{\text{cond},\tilde{\mathcal{H}}_{\text{cond},0}}(t) = -\frac{1}{2} \sum_{j,\sigma} g_{L,j} \sum_{n_j=0}^{\infty} \int \frac{dk_{j,\parallel}}{2\pi} e^{i\sigma(\omega_0 - \tilde{\omega}'_{j,e})(t-t_0)} \tilde{\psi}_{j,n_j,\sigma}^\dagger(k_{j,\parallel}, t_0) \tilde{\Omega}'_{j,e} \tilde{\psi}_{j,n_j,-\sigma}(k_{j,\parallel}, t_0). \quad (55)$$

We note that all three of these transformed Hamiltonians correspond to spin-dependent external field interactions, where the fields are

$$U_{n,i,i';m_l,m'_l}(t) = -\frac{\Omega_n}{2} \delta_{i,i'} \sum_{\sigma=\pm 1} \delta_{m'_l, m_l + \sigma} A_{I,m_l}^\sigma e^{i\sigma(\omega_0 - \omega_n)(t-t_0)}, \quad (56)$$

$$U_{e,i,i';q,q'}(t) = -\frac{\Omega_e}{2} \delta_{i,i'} \delta_{q,q'} \delta_{\sigma', -\sigma} e^{i\sigma(\omega_0 - \omega_e)(t-t_0)}, \quad (57)$$

$$U_{\text{cond},j,j';n_j,n'_j}(t) = -\frac{\tilde{\Omega}'_{j,e}}{2} \delta_{j,j'} \delta_{n_j,n'_j} \delta_{k_{j,\parallel}, k'_{j,\parallel}} \delta_{\sigma', -\sigma} e^{i\sigma(\omega_0 - \tilde{\omega}'_{j,e})(t-t_0)}, \quad (58)$$

Then, we time transform the difficult (interaction) parts of the full Hamiltonian. The hyperfine and local electron-electron interactions are elementary to transform. We obtain

$$\begin{aligned} \mathcal{H}_{hf, \mathcal{H}_{n,0} + \mathcal{H}_{e,0}}(t) &= -\frac{D_z}{4} \sum_{i,q,\sigma,m_l} m_l \sigma a_{i,m_l}^\dagger(t_0) a_{i,m_l}(t_0) b_{i,q,\sigma}^\dagger(t_0) b_{i,q,\sigma}(t_0) \\ &\quad - \frac{D_x}{2} \sum_{i,q,\sigma,m_l} A_{I,m_l}^\sigma e^{i\sigma(\omega_e - \omega_n)(t-t_0)} a_{i,m_l+\sigma}^\dagger(t_0) a_{i,m_l}(t_0) b_{i,q,-\sigma}^\dagger(t_0) b_{i,q,\sigma}(t_0), \end{aligned} \quad (59)$$

$$\mathcal{H}_{e,\text{int}, \mathcal{H}_{e,0}}(t) = \frac{1}{2} \sum_{i,q,\sigma} U_q \hat{n}_{i,q,\sigma}(t_0) \hat{n}_{i,q,-\sigma}(t_0), \quad (60)$$

Of these, only the transverse (D_x) part of the hyperfine interaction picks up a time dependence. Before we time transform the remaining two interaction Hamiltonians, we first spatially transform the conduction electron operators in the presence of the magnetic field necessary for the NMR experiment. Then we rewrite $\mathcal{H}_{e,\text{cond}}$ in terms of the spatially-transformed conduction electron fields,

$$\mathcal{H}_{e,\text{cond}} \rightarrow \tilde{\mathcal{H}}_{e,\text{cond}} = \sum_{i,q,j} g_{L,j} \sum_{n_j=0}^{\infty} \int \frac{dk_{j,\parallel}}{2\pi} \left(v_{i,q,j} \tilde{\psi}_{j,n_j,\sigma}^\dagger(k_{j,\parallel}) b_{i,q,\sigma} + H.c. \right), \quad (61)$$

which after time-transformation with respect to $\mathcal{H}_{e,0}$ and $\tilde{\mathcal{H}}_{\text{cond},0}$ becomes

$$\begin{aligned} \tilde{\mathcal{H}}_{e,\text{cond}, \mathcal{H}_{e,0} + \tilde{\mathcal{H}}_{\text{cond},0}}(t) &= \sum_{i,q,j} g_{L,j} \sum_{n_j=0}^{\infty} \int \frac{dk_{j,\parallel}}{2\pi} \left(v_{i,q,j} e^{i[\varepsilon_j(n_j, k_{j,\parallel}) - \varepsilon_q + \sigma(\omega_e - \tilde{\omega}'_{j,e})/2](t-t_0)} \right. \\ &\quad \left. \tilde{\psi}_{j,n_j,\sigma}^\dagger(k_{j,\parallel}, t_0) b_{i,q,\sigma}(t_0) + H.c. \right) \end{aligned} \quad (62)$$

The most important Hamiltonian for the Knight shift in a superconductor is the pairing interaction \mathcal{H}_{sc} , which in position space was written in Equation (10). Since in a Knight shift measurement, the experimenter first measures the Knight shift in the applied field $\mathbf{H}(t)$ and hence the induction

$\mathbf{B}(t) = \mu_0 \mathbf{H}(t)$ while the superconductor is in its normal (metallic) state, and then cools the material through its superconducting transition at $T_c(H)$, it is clear that the correct formulation for the superconducting pairing interaction must be in momentum space, and more precisely, to account for the pairing of the electrons (or holes) while they are in Landau orbits in the normal state. We therefore first rewrite \mathcal{H}_{sc} in a fully spatially-transformed magnetic-induction-quantized form that allows for different pairing interactions, such as those giving rise to various types of spin-singlet and spin-triplet superconductors arising from a multiple-band metal. As a start to understand the orbital motion of the paired superconducting electrons (or holes), we first assume the standard approximation for the evaluation of the upper critical field H_{c2} that the paired particles of combined charge $2e$ move together in Landau levels [18,42,52,53]. For a BCS superconductor for which $V_{j,j';\sigma,\sigma'}(\mathbf{k}_j - \mathbf{k}'_{j'}) = -V_0 \delta_{j,j'} \delta_{\sigma,-\sigma'}$, there is no need to transform the wave vector dependence of the pairing interaction due to the Landau orbits formed by the strong applied field [18]. Such pairing interactions will be considered elsewhere. Thus, we begin by considering only the simplest case of isotropic intraband pairing of equivalent strength in all of the bands, which after spatial transformation due to the magnetic induction may be written as

$$\tilde{H}_{sc,0} = -V_0 \sum_{\sigma} \sum_j g_{L,j}^2 \sum_{n_j, n'_j=0}^{\infty} \int \frac{dk_{j,\parallel}}{2\pi} \int \frac{dk'_{j,\parallel}}{2\pi} \tilde{\psi}_{j,n_j,\sigma}^{\dagger}(k_{j,\parallel}) \tilde{\psi}_{j,n_j,-\sigma}^{\dagger}(-k_{j,\parallel}) \tilde{\psi}_{j,n'_j,-\sigma}(-k'_{j,\parallel}) \tilde{\psi}_{j,n'_j,\sigma}(k'_{j,\parallel}), \quad (63)$$

and transforming this in time using $\mathcal{H}_{cond,0}$, we have

$$\begin{aligned} \tilde{H}_{sc,0, \tilde{H}_{cond,0}}(t) = & -V_0 \sum_{\sigma} \sum_j g_{L,j}^2 \sum_{n_j, n'_j=0}^{\infty} \int \frac{dk_{j,\parallel}}{2\pi} \int \frac{dk'_{j,\parallel}}{2\pi} \tilde{\psi}_{j,n_j,\sigma}^{\dagger}(k_{j,\parallel}, t_0) \tilde{\psi}_{j,n_j,-\sigma}^{\dagger}(-k_{j,\parallel}, t_0) \\ & \times \tilde{\psi}_{j,n'_j,-\sigma}(-k'_{j,\parallel}, t_0) \tilde{\psi}_{j,n'_j,\sigma}(k'_{j,\parallel}, t_0), \end{aligned} \quad (64)$$

which is independent of t .

5. Dyson's Equations for the Green Functions

For a system with continuous position variables \mathbf{r} , the contour C Dyson equation for an adiabatic time-dependent interaction for which $C_{int} \rightarrow C$ can be written as [44]

$$\begin{aligned} G(1,1') = & G_0(1,1') + \int d^3 \mathbf{r}_2 \int_C d\tau_2 G_0(1,2) U(2) G(2,1') \\ & + \int d^3 \mathbf{r}_2 \int d^3 \mathbf{r}_3 \int_C d\tau_2 \int_C d\tau_3 G_0(1,2) \Sigma(2,3) G(3,1'), \end{aligned} \quad (65)$$

where Σ is the self-energy and U is an external field. By carefully keeping the order of the times in going about the contour C , one can analytically continue the integrals off the real axis to the real axis. We first need to define the retarded and advanced Green functions, which are

$$G^r(1,1') = \Theta(t_1 - t_{1'}) [G^>(1,1') - G^<(1,1')], \quad (66)$$

$$G^a(1,1') = \Theta(t_{1'} - t_1) [G^<(1,1') - G^>(1,1')], \quad (67)$$

Then, letting $\int_C d\tau_2 G_0(1,2) G(2,1')$ be represented by $C = AB$, one can analytically continue the appropriate contour-ordered Green function components on the real axis, so that

$$C^< = A^r B^< + A^< B^a, \quad (68)$$

$$C^> = A^r B^> + A^> B^a, \quad (69)$$

where the integration $\int_C d\tau_2 \rightarrow \int_{-\infty}^{\infty} dt_2$. Similarly, by representing the double contour integral $\int_C d\tau_2 \int_C d\tau_3 G_0(1,2)\Sigma(2,3)G(3,1')$ by $D = ABC$, one can analytically continue these contour integration paths to the real axis, obtaining [44]

$$D^< = A^r B^r C^< + A^r B^< C^a + A^< B^a C^a, \quad (70)$$

$$D^> = A^r B^r C^> + A^r B^> C^a + A^> B^a C^a, \quad (71)$$

We then implement the three Dyson equations for the nuclear, local orbital electron, and conduction electron Green functions. We first consider the Dyson equation for the nuclear Green function. In this case, there are two terms to consider: the external field U_n given by Equation (56), and the hyperfine interaction given by Equation (59). However, the hyperfine interaction does not involve two different times, as in the self-energy, which is analogous to the exchange interaction in the electron gas with electron-electron Coulomb interactions. It is instead analogous to the direct interaction with a fermion loop, but in this case, the fermion loop is for the local orbital electrons. As first shown by Hall and Klemm, the leading self-energy diagrams for the Knight shift and the linewidth changes in a metal at $T = 0$ are shown in Figure 3.

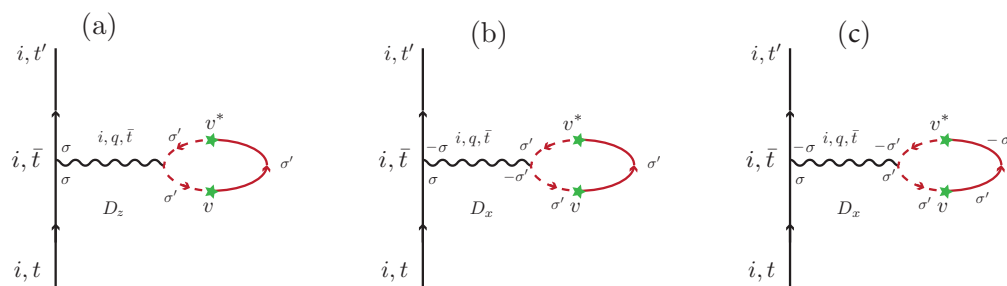


Figure 3. Hall-Klemm diagrams for the Knight shift linewidth changes at $T = 0$. The vertical solid lines on the left are the nuclear $G_n(1,1')$, the wiggly horizontal line represents the hyperfine interaction, the dashed curves represent G_e , the stars represent the excitation from the local orbitals to the conduction band, and the solid counterclockwise arrowed curves represent the conduction electron G_{cond} . (a) represents the leading Knight shift contribution arising from D_z ; (b,c) represent the two leading contributions to the linewidth changes arising from D_x [43]. Reprinted with permission of B. E. Hall and R. A. Klemm. Microscopic model of the Knight shift in anisotropic and correlated metals. *J. Phys. Condens. Matter* **2016**, *28*, 03LT01. Copyright©2016 Institute of Physics.

6. Proposed Calculation of $K(T)$ in the Normal and Superconducting States

6.1. Gor'kov's Derivation of the Ginzburg-Landau Equations

Since the upper critical field has been obtained for anisotropic superconductors with a variety of pairing interactions [18,42,52,53] and also that the most rapid temperature variation, a discontinuity in slope, of the conventional Knight shift in superconductors, occurs just at the superconducting transition, it is evident that an extension of those upper critical field calculations to the Ginzburg-Landau regime just below $T_{c2}(\mathbf{B}_0)$ can provide the crucial information for $K_S(T)$ in the superconducting state. We propose to extend the Hall-Klemm $T = 0$ Knight shift calculation in the presence of a strong magnetic induction $B(t)$ into the superconducting state using an extension of the microscopic derivation of the Ginzburg-Landau expression for the gap function as pioneered by Gor'kov [54,55] to include the time-dependent applied field. That work was generalized for a general $V(\mathbf{r} - \mathbf{r}')$

single-band pairing by Scharnberg and Klemm [18]. In the superconducting state, we require the regular (conduction) and anomalous Green functions

$$G_{j,j';\sigma,\sigma'}(1,1') = -i\langle T_C[\psi_{j,\sigma,\mathcal{H}}(1)\psi_{j',\sigma',\mathcal{H}}^\dagger(1')] \rangle, \quad (72)$$

$$F_{j,j';\sigma,\sigma'}(1,1') = \langle T_C[\psi_{j,\sigma,\mathcal{H}}(1)\psi_{j',\sigma',\mathcal{H}}(1')] \rangle, \quad (73)$$

$$F_{j,j';\sigma,\sigma'}^\dagger(1,1') = \langle T_C[\psi_{j,\sigma,\mathcal{H}}^\dagger(1)\psi_{j',\sigma',\mathcal{H}}^\dagger(1')] \rangle, \quad (74)$$

and the gap function, which in real space for intraband pairing only is

$$\Delta_{j,\sigma,\sigma'}(\mathbf{r}_j, \mathbf{r}'_j) = V_j(\mathbf{r}_j - \mathbf{r}'_j)\delta_{j,j'}F_{j,j';\sigma,\sigma'}(1,1')|_{t_1-t_1'=0^+}, \quad (75)$$

As discussed in the next subsection, in order to include the temperature dependence of the normal state of the nuclei, the local orbital electrons, and the conduction electrons, we need to quantize the conduction electrons in momentum space and Landau orbits, as was done for the bare conduction electron Green functions in Equations (42) and (43). Although this was never done in upper critical field calculations [17,18,32,42,48,49,52,53], the reasons given for not doing it were that impurities would broaden the levels, smearing out the Landau level spacings [18,52]. However, with the present quality of some materials, that argument should be reexamined. More important, in order to calculate the upper critical induction B_{c2} , one requires the paired electrons (or holes) to be in Landau levels [17,18,32,42,48,49,52,53]. However, as discussed in the next section, it is not clear that electrons (or holes) will only pair with other electrons (or holes) in the same Landau orbit. With multiple bands, an electron in one single-particle Landau level corresponding to one conduction band could in principle pair with another electron in a different Landau level corresponding to another band. So one will have to make some assumptions about the pairing processes to simplify the calculations. However, to get a preliminary microscopic idea of how $K_S(T)$ picks up its T dependence below T_c , we will first revisit the Gor'kov procedure for deriving the Ginzburg-Landau equations in real space.

In the standard real-space finite temperature formalism, the Gor'kov equations of motion generalized to include multiple ellipsoidally anisotropic bands and their Zeeman energies without interband pairing are [18]

$$\begin{aligned} \left(i\omega_n - \sum_{\nu=1}^3 \frac{1}{2m_{j,\nu}} [\nabla_{j,\nu}/i - e\mathbf{A}_{j,\nu}(\mathbf{r}_j)]^2 + \mu - \sigma\omega'_{j,e}/2 \right) G_{j,j';\sigma,\sigma'}(\mathbf{r}_j, \mathbf{r}'_j, \omega_n) \\ + \sum_{\rho} \int d^3\mathbf{r}''_j \Delta_{j,\sigma,\rho}(\mathbf{r}_j, \mathbf{r}''_j) F_{j,j';\rho,\sigma'}^\dagger(\mathbf{r}''_j, \mathbf{r}'_j, \omega_n) = \delta_{\sigma,\sigma'} \delta_{j,j'} \delta^{(3)}(\mathbf{r}_j - \mathbf{r}'_j), \end{aligned} \quad (76)$$

$$\begin{aligned} \left(-i\omega_n - \sum_{\nu=1}^3 \frac{1}{2m_{j,\nu}} [\nabla_{j,\nu}/i + e\mathbf{A}_{j,\nu}(\mathbf{r}_j)]^2 + \mu - \sigma\omega'_{j,e}/2 \right) F_{j,j';\sigma,\sigma'}^\dagger(\mathbf{r}_j, \mathbf{r}'_j, \omega_n) \\ + \sum_{\rho} \int d^3\mathbf{r}''_j \Delta_{j,\sigma,\rho}^*(\mathbf{r}_j, \mathbf{r}''_j) G_{j,j';\rho,\sigma'}(\mathbf{r}''_j, \mathbf{r}'_j, \omega_n) = 0, \end{aligned} \quad (77)$$

where $\omega_n = (2n + 1)\pi/\beta$ is the fermion Matsubara frequency. Letting $G_{j,j';\sigma,\sigma'}^{(0)}(\mathbf{r}_j, \mathbf{r}'_j, \omega_n)$ be the solution for the G function in the normal state with $\Delta = 0$, one can rewrite the above equations for G and F^\dagger in the finite temperature formalism as

$$\begin{aligned} G_{j,j';\sigma,\sigma'}(\mathbf{r}_j, \mathbf{r}'_j, \omega_n) = G_{j,j';\sigma,\sigma'}^{(0)}(\mathbf{r}_j, \mathbf{r}'_j, \omega_n) \delta_{j,j'} \delta_{\sigma,\sigma'} \\ - \sum_{\rho} \int d^3\mathbf{r}''_j \int d^3\mathbf{r}'''_j G_{j,j';\sigma,\sigma'}^{(0)}(\mathbf{r}_j, \mathbf{r}'''_j, \omega_n) \Delta_{j,\rho,\sigma}(\mathbf{r}''_j, \mathbf{r}'_j) \\ \times \int d^3\boldsymbol{\xi}_j \int d^3\boldsymbol{\xi}'_j \sum_{\rho'} G_{j,j';\sigma',\sigma'}^{(0)}(\mathbf{r}'_j, \boldsymbol{\xi}'_j, -\omega_n) \Delta_{j,\rho',\sigma'}^*(\boldsymbol{\xi}_j, \boldsymbol{\xi}'_j) G_{j,\rho,\rho'}^{(0)}(\mathbf{r}''_j, \boldsymbol{\xi}_j, \omega_n), \end{aligned} \quad (78)$$

to order Δ^2 . One can then substitute this into the equation for F^\dagger , multiply by the pairing interaction, and obtain a self-consistent equation for Δ to order Δ^3 [54,55]. The coefficients of the two terms proportional to Δ define the upper critical induction B_{c2} [18,32,42,48,49,52,53]. Functionally integrating the cubic equation with respect to $\Delta_{j,\sigma,\sigma'}(r_j, r'_j)$ and by neglecting the field dependence of the resulting term proportional to $|\Delta|^4$, one can obtain the generalized Ginzburg-Landau free energy.

We note that even if one completely neglects the field dependence of the term of order Δ^3 in the Gor'kov expansion of F^\dagger for $\Delta(r)$, it is easy to see that this procedure will lead to the following phenomenological general result:

$$K_S(T) = a(\mathbf{B}_0) - b(\mathbf{B}_0)|\Delta(\mathbf{B}_0, T)|^2, \quad (79)$$

where a and b strongly depend upon the magnitude and direction of \mathbf{B}_0 , but not much upon T , and $2|\Delta(\mathbf{B}_0, T)|$ is the effective superconducting gap in the Ginzburg-Landau regime. This simple result includes the pairing in all of the bands, which couple together to give one effective $T_{c2}(\mathbf{B}_0)$, below which $|\Delta(\mathbf{B}_0, T)|^2 \propto [T_{c2}(\mathbf{B}_0) - T]$. It remains to be seen if this form could be generalized to the full BCS superconducting gap $|\Delta(\mathbf{B}_0, T)|$ temperature dependence, which saturates at low T values. If so, it could lead to a quantitative theory of the Knight shift that would be valid for essentially any type of superconductor involving Cooper pairing. Hence, a proper calculation of $a(\mathbf{B}_0)$ and $b(\mathbf{B}_0)$ can provide a microscopic understanding of the behavior for the $^{63}\text{CuO}_2$ $K_S(T)$ for \mathbf{B}_0 parallel and normal to the layers of $\text{YBa}_2\text{Cu}_3\text{O}_{7-\delta}$, which was described by Slichter as “fortuitous” [20]. It could in principle explain the small or vanishing b term in Sr_2RuO_4 , at least for the field normal to the layers, for which Landau level formation would be highly restricted on two of the Fermi surfaces.

6.2. High-Field Solution for an Anisotropic, Multiband Type-II BCS Superconductor

More important, we note that a major simplification of the Keldysh contour procedure can be made by first taking the mean-field approximation of the BCS pairing interaction represented in momentum space by Equation (63). We write the mean-field gap (or isotropic order parameter) for singlet pairing in band j as

$$\Delta_{j,-\sigma,\sigma} = V_{0g_{L,j}} \sum_{n_j=0}^{\infty} \int \frac{dk_{j,\parallel}}{2\pi} \langle \tilde{\psi}_{j,n_j,-\sigma}(-k_{j,\parallel}) \tilde{\psi}_{j,n_j,\sigma}(k_{j,\parallel}) \rangle, \quad (80)$$

where the expectation value is in the grand canonical ensemble, so that the mean-field effective Hamiltonian for the conduction electrons in the superconducting state becomes

$$\begin{aligned} \tilde{\mathcal{H}}_{\text{sc,cond}} = & \sum_{j,\sigma} g_{L,j} \sum_{n_j=0}^{\infty} \int \frac{dk_{j,\parallel}}{2\pi} \left(\tilde{\psi}_{j,n_j,\sigma}^\dagger(k_{j,\parallel}) [\varepsilon_j(n_j, k_{j,\parallel}) - \mu_{\text{cond,cp}} - \sigma \tilde{\omega}'_{j,e}/2] \tilde{\psi}_{j,n_j,\sigma}(k_{j,\parallel}) \right. \\ & \left. + [\tilde{\psi}_{j,n_j,\sigma}^\dagger(k_{j,\parallel}) \tilde{\psi}_{j,n_j,-\sigma}^\dagger(-k_{j,\parallel}) \Delta_{j,-\sigma,\sigma} + H.c.] \right) \end{aligned} \quad (81)$$

where we have included the chemical potential of the conduction electrons. Note that we assume the total momentum of the paired electrons (or holes) is zero, as both are assumed to be on opposite sides of the same Landau orbit, and have opposite momenta in the direction normal to the plane of the Landau orbits. This effective quadratic Hamiltonian can then be diagonalized by a standard Bogoliubov-Valatin transformation [56], letting

$$\tilde{\psi}_{j,n_j,\uparrow}(k_{j,\parallel}) = u_{j,n_j,k_{j,\parallel}} \gamma_{j,n_j,\uparrow}(k_{j,\parallel}) + v_{j,n_j,k_{j,\parallel}} \gamma_{j,n_j,\downarrow}^\dagger(k_{j,\parallel}), \quad (82)$$

$$\tilde{\psi}_{j,n_j,\downarrow}^\dagger(-k_{j,\parallel}) = -v_{j,n_j,k_{j,\parallel}}^* \gamma_{j,n_j,\uparrow}(k_{j,\parallel}) + u_{j,n_j,k_{j,\parallel}}^* \gamma_{j,n_j,\downarrow}^\dagger(k_{j,\parallel}), \quad (83)$$

where we require the γ operators to obey independent fermion statistics. Using the standard transformation procedure to eliminate the off-diagonal terms, we then obtain

$$|u_{j,n_j,k_{j,\parallel}}|^2 = \frac{1}{2} \left[1 + \left(\frac{\varepsilon_j(n_j, k_{j,\parallel}) - \mu_{\text{cond,cp}}}{E_j(n_j, k_{j,\parallel})} \right) \right], \quad (84)$$

$$|v_{j,n_j,k_{j,\parallel}}|^2 = \frac{1}{2} \left[1 - \left(\frac{\varepsilon_j(n_j, k_{j,\parallel}) - \mu_{\text{cond,cp}}}{E_j(n_j, k_{j,\parallel})} \right) \right], \quad (85)$$

and the diagonalized superconducting Hamiltonian becomes

$$\tilde{\mathcal{H}}_{\text{sc,cond}} \rightarrow \sum_{j,\sigma} g_{L,j} \sum_{n_j=0}^{\infty} \int \frac{dk_{j,\parallel}}{2\pi} \gamma_{j,n_j,\sigma}^\dagger(k_{j,\parallel}) \gamma_{j,n_j,\sigma}(k_{j,\parallel}) \left[E_j(n_j, k_{j,\parallel}) + \sigma \tilde{\omega}'_{j,e}/2 \right], \quad (86)$$

$$E_j(n_j, k_{j,\parallel}) = \sqrt{[\varepsilon_j(n_j, k_{j,\parallel}) - \mu_{\text{cond,cp}}]^2 + |\Delta_j|^2}, \quad (87)$$

where $|\Delta_j|^2 = \Delta_{j,-\sigma,\sigma} \Delta_{j,-\sigma,\sigma}^\dagger$ is positive definite for each j value. We note that the quasiparticle dispersions in $\tilde{\mathcal{H}}_{\text{sc,cond}}$ are nearly identical to the BCS quasiparticle dispersions, as they do indeed have a real energy gap $2|\Delta|$, but there is in addition an effective Zeeman term arising from the difference in the spin up and spin down quasiparticle energies, leading to a magnetic gap function. Thus, the self-consistent expression from Equation (80) for $\Delta_{j,-\sigma,\sigma}$ becomes

$$\Delta_{j,\downarrow,\uparrow} = -V_0 g_{L,j} \sum_{\sigma=\pm} \sum_{n_j=0}^{\infty} \int \frac{dk_{j,\parallel}}{2\pi} \frac{\Delta_{j,\downarrow,\uparrow}}{E_j(n_j, k_{j,\parallel})} \left(\frac{1}{e^{\beta[E_j(n_j, k_{j,\parallel}) + \sigma \tilde{\omega}'_{j,e}/2]} + 1} - \frac{1}{2} \right), \quad (88)$$

which, combined with Equation (86), explicitly demonstrates the presence of the superconducting gap Δ_j in each band that is involved in $K_S(T)$ in the superconducting state. Thus, it is clear that the effective or phenomenological Equation (79) mentioned in the abstract for $K_S(T)$ applies in the mixed state of a type-II superconductor, not just in the Ginzburg-Landau region. However, by quantizing the superconducting order parameter at a finite induction strength B_0 , both the Landau orbits and the Zeeman interaction can greatly affect its B_0 dependence, and the Landau orbits in particular can be distinctly different for layered compounds with B_0 parallel or perpendicular to the layers, especially at large induction strengths, as first noted in experiments on $\text{YBa}_2\text{Cu}_3\text{O}_{7-\delta}$ [19,20].

The road ahead to construct the first microscopic theory of the Knight shift in a superconductor of any type is now clear. The conduction electrons must be quantized in Landau orbits, and this can be done for any number of ellipsoidally anisotropic electron or hole bands, as outlined above. The procedure will be extended for our model of multiple ellipsoidal bands with the Zeeman couplings and time-dependent Zeeman couplings in each band to construct the Bogoliubov-Valatin transformed contour G functions. To do this properly, one needs to apply those transformations presented in Equations (82) and (83) to the time-dependent Zeeman interaction on the conduction electrons in Equation (44) and also to the Anderson-like interaction in Equation (61) that removes a local orbital electron and places it in the superconducting state and *vice versa*. This will cause Equations (44), (55), (61) and (62) to be rewritten in terms of the quasiparticle operators $\gamma_{j,n_j,\sigma}(k_{j,\parallel})$ and $\gamma_{j,n_j,\sigma}^\dagger(k_{j,\parallel})$, and will modify Equation (58). Then, the Keldysh contour method can be used to perform a microscopic theory of $K_S(T)$ in the mixed superconducting state of an anisotropic, multiband, type-II BCS superconductor. Since the conduction electrons are transformed into non-interacting quasiparticles in the superconducting state, the self-energy $\Sigma(2,3)$ in Dyson's equation will only apply to the orbital electrons via the Hubbard interaction U_q . All other interactions reduce to effective external fields. After a detailed microscopic evaluation of $K_S(T)$ using the contour-extended version of the diagram pictured in Figure 3a, special attention will be directed at the conditions for a near vanishing of $b(B_0)$, which could lead to a T -independent $K_S(T)$, even for a "conventional" superconductor. The linewidth

changes can be evaluated in the superconducting state from the contour-extended versions of the diagrams pictured in Figure 3b,c. Eventually, other superconducting pairing symmetries could also be studied with this technique, although the pairing interaction would have to be transformed as above, including the Landau orbits. Eventually, this could be done for charge-density and spin-density wave systems, for which no theory of the Knight shift is presently available. We note that $2H-TaS_2$ has a nodal charge-density wave below 75 K, with a presumably s -wave superconducting state entering below 0.6 K [17,57], which is very similar to the complex situation in the high-temperature superconductor $Bi_2Sr_2CaCu_2O_{8+\delta}$, in which the nodal pseudogap (probably charge-density wave) regions and isotropic s -wave superconducting regions break up into spatial domains [58]. These results are consistent with previous c -axis twist Josephson junction experiments on that material [59]. Although the NMR linewidths in that material are too broad to perform Knight shift measurements, they could be done on other materials, such as the dichalcogenides, and also in improved $YBa_2Cu_3O_{7-\delta}$ samples.

7. Discussion and Conclusions

We have outlined a procedure to obtain a microscopic theory of the Knight shift in an anisotropic Type-II superconductor. This was based upon the Hall-Klemm microscopic model of the effect at $T = 0$ [43], for which multiple anisotropic conduction bands of ellipsoidal shapes were included. We considered the simplest magnetic resonance case of $\mathbf{B}(t) = \mathbf{B}_0 + \mathbf{B}_1(t)$ with $|\mathbf{B}_1| \ll |\mathbf{B}_0|$ and $\mathbf{B}_1 \cdot \mathbf{B}_0 = 0$ with $\mathbf{B}_1(t)$ oscillating at a single frequency ω_0 . For this simple case, the time changes to the system are adiabatic, so that the interaction Keldysh contour C_{int} shown in Figure 1b effectively coincides with contour C depicted in Figure 1a, and the integrations can be analytically continued onto the real axis. The procedure can effectively treat any nuclear spin value I . The conduction electrons (or holes) were quantized in Landau orbits in the applied field in the normal state, and the Hamiltonian for a generalized anisotropic, multiband BCS type-II superconductor was diagonalized, allowing for a full treatment of the superconducting state.

We emphasize that by quantizing the superconducting order parameter in the presence of a strong time-independent magnetic induction \mathbf{B}_0 , the energy spacings of the Landau orbits can depend strongly upon the direction of \mathbf{B}_0 . At very weak \mathbf{B}_0 values, the Landau levels primarily give rise to overall anisotropic constant backgrounds of $K(T)$ and $K_S(0)$, with $K_S(T)$ being predominantly governed by the anisotropic Zeeman interactions and D_z . However, for sufficiently strong \mathbf{B}_0 values in anisotropic materials with layered or quasi-two-dimensional anisotropy, the spacings between the Landau energy levels depends strongly upon the direction of \mathbf{B}_0 , so that $K_S(T)$ could become independent of T for $T \leq T_c$, as first observed for $\mathbf{B}_0 \parallel \hat{c}$ in $YBa_2Cu_3O_{7-\delta}$ [19,20]. Such behavior could also arise for quasi-one-dimensional materials in all \mathbf{B}_0 directions, although to different degrees for \mathbf{B}_0 parallel and perpendicular to the most conducting crystal direction.

Since the crucial interaction for the Knight shift is the hyperfine interaction between the probed nuclei and their surrounding orbital electrons, the symmetry of this interaction can be very important. Generally, the hyperfine interaction can arise from the electrons in any of the orbital levels. For s -orbitals, the Fermi contact term is important, but the induced-dipole induced-dipole interactions can arise from the nucleus of any spin for any spin $I \geq 1/2$ and its surrounding electrons in any orbital, and induced-quadrupole induced-quadrupole and higher order interactions can also occur for certain orbitals and nuclear spin values [60,61]. In the Hall-Klemm model [43], the hyperfine interaction crucial for the Knight shift was taken to be diagonal in the spin representations of a lattice with tetragonal symmetry $D_x = D_y \neq D_z$. In that simple model, the $T = 0$ results indicated that the Knight shift arose from D_z , and the line width was modified by $D_x = D_y$. In more realistic examples of correlated and anisotropic materials, the hyperfine interaction would be represented by a symmetric matrix unless time-reversal symmetry-breaking interactions were present. Such matrices can be diagonalized by a set of rotations, but in complicated cases the quantization axes would not necessarily be the same as for the overall crystal structure. Such complications would mix the Knight shift and its linewidth, depending upon the direction of \mathbf{B}_0 .

As noted previously, in first quantization, an isolated nuclear spin wave function in an NMR experiment was found to have the form

$$|I, m_I\rangle(t) = e^{im_I\omega_0 t} \sum_{m'_I=-I}^I C_{m'_I}^{m_I} e^{im'_I\Gamma_n t}, \quad (89)$$

where $\Gamma_n = [(\omega_0 - \omega_n)^2 + \Omega_n^2]^{1/2}$ is the nuclear resonance function and the constants $C_{m'_I}^{m_I}$ depend upon the initial conditions [43]. Those authors found this form to hold for $I = 1/2, 1, 3/2$, and in second quantization, up to $I = 2$, so it is likely to hold for arbitrary I . In the adiabatic regime, we have $\omega_0 \ll \omega_n$ [37,38], so that there will be a manifold of geometrical phases that will arise with higher I values.

We remark that it is possible to generalize this treatment to more complicated $B_1(t)$ functions, such as a periodic function of square-wave or triangle-wave shape. This can be represented as a Fourier series, but if the primary angular frequency is ω_0 , terms of higher multiples n of ω_0 can be present, some of which would violate the adiabatic requirement that they be much smaller than the Zeeman energy spacings. Hence, this experiment would make some amount of non-adiabatic changes that could drive the system out of thermal equilibrium, and the two contours C and C_{int} shown in Figure 1 and discussed above would not coincide, greatly complicating the analysis.

Conflicts of Interest: The authors declare no conflict of interest.

References

1. Knight, W.D. Nuclear magnetic resonance shift in metals. *Phys. Rev.* **1949**, *76*, 1259–1260.
2. Knight, W.D.; Androes, G.M.; Hammond, R.H. Nuclear magnetic resonance in a superconductor. *Phys. Rev.* **1956**, *104*, 852–853.
3. Reif, F. Observation of nuclear magnetic resonance in superconducting mercury. *Phys. Rev.* **1956**, *102*, 1417–1418.
4. Reif, F. The study of superconducting Hg by nuclear magnetic resonance techniques. *Phys. Rev.* **1957**, *106*, 208–221.
5. Yosida, K. Paramagnetic susceptibility in superconductors. *Phys. Rev.* **1958**, *110*, 769–770.
6. Gladstone, G.; Jensen, M.A.; Schrieffer, J.R. Superconductivity in the transition metals. In *Superconductivity*; Parks, R.D., Eds.; Marcel Dekker, Inc.: New York, NY, USA, 1969; pp. 801–803.
7. Abrikosov, A.A.; Gor'kov, L.P. Spin-orbit interaction and the Knight shift in superconductors. *Sov. Phys. JETP* **1962**, *15*, 752–757.
8. Baek, S.-H.; Harnegea, L.; Wurmehl, S.; Büchner, B.; Grafe, H.-J. Anomalous superconducting state in LiFeAs implied by the ^{75}As Knight shift measurement. *J. Phys. Condens. Matter* **2013**, *25*, 162204, doi:10.1088/0953-8984/25/16/162204.
9. Kohori, Y.; Yamato, Y.; Iwamoto, Y.; Kohara, T.; Bauer, E.D.; Maple, M.B.; Sarrao, J.L. NMR and NQR studies of the heavy fermion superconductors CeTIn₅ (T = Co and Ir). *Phys. Rev. B* **2001**, *64*, 134526, doi:10.1103/PhysRevB.64.134526.
10. Lee, I.J.; Brown, S.E.; Clark, W.G.; Strouse, M.J.; Naughton, M.J.; Kang, W.; Chaikin, P.M. Triplet superconductivity in an organic superconductor probed by NMR Knight shift. *Phys. Rev. Lett.* **2002**, *88*, 17004, doi:10.1103/PhysRevLett.88.17004.
11. Lee, I.J.; Brown, S.E.; Clark, W.G.; Strouse, M.J.; Naughton, M.J.; Chaikin, P.M.; Brown, S.E. Evidence from ^{77}Se Knight shifts for triplet superconductivity in $(\text{TMTSF})_2\text{PF}_6$. *Phys. Rev. B* **2003**, *68*, 092510, doi:10.1103/PhysRevB.68.092510.
12. Michioka, C.; Ohta, H.; Itoh, Y.; Yoshimura, K.; Kato, M.; Sakurai, H.; Takayama-Muromachi, E.; Takada, K.; Sasaki, T. Knight shift of triangular lattice superconductor $\text{Na}_{0.35}\text{CoO}_2 \cdot 1.3\text{H}_2\text{O}$. *Phys. B* **2006**, *628–629*, doi:10.1016/j.physb.2006.01.181.

13. Kato, M.; Michioka, C.; Waki, T.; Itoh, Y.; Yoshimura, K.; Ishida, K.; Sakurai, H.; Takayama-Muromachi, E.; Takada, K.; Sasaki, T. Possible spin triplet superconductivity in $\text{Na}_x\text{CoO}_2 \cdot y\text{H}_2\text{O}$: ^{59}Co NMR Studies. *J. Phys. Condens. Matter* **2006**, *18*, 669–682.
14. Sakurai, H.; Ihara, Y.; Takada, K. Superconductivity of cobalt oxide hydrate $\text{Na}_x(\text{H}_3\text{O})_z\text{CoO}_2 \cdot y\text{H}_2\text{O}$. *Phys. C* **2015**, 378–387, doi:10.1016/j.physc.2015.02.010.
15. Klemm, R.A. Striking similarities between the pseudogap phenomenon in the cuprates and in layered organic and dichalcogenide superconductors. *Physica C* **2000**, 341–348, 839–842.
16. Chou, F.C.; Cho, J.H.; Lee, P.A.; Abel, E.T.; Matan, K.; Lee, Y.S. Thermodynamic and transport measurements of superconducting $\text{Na}_{0.3}\text{CoO}_2 \cdot 1.3\text{H}_2\text{O}$ single crystals prepared by electrochemical deintercalation. *Phys. Rev. Lett.* **2004**, *92*, 157004, doi:10.1103/PhysRevLett.92.157004.
17. Klemm, R.A. *Layered Superconductors Volume 1*; Oxford University Press: Oxford, UK, 2012.
18. Scharnberg, K.; Klemm, R.A. *P-Wave superconductors in magnetic fields*. *Phys. Rev. B* **1980**, *22*, 5233–5244.
19. Barrett, S.E.; Durand, D.J.; Pennington, C.H.; Slichter, C.P.; Friedmann, T.A.; Rice, J.P.; Ginsberg, D.M. ^{63}Cu Knight shifts in the superconducting state of $\text{YBa}_2\text{Cu}_3\text{O}_{7-\delta}$ ($T_c = 90$ K). *Phys. Rev. B* **1990**, *41*, 6283–6296.
20. Slichter, C.P. The Knight shift — A powerful probe of condensed-matter systems. *Philos. Mag. Part B* **1999**, *79*, 1253–1261.
21. Fujiwara, K.; Kitaoka, Y.; Ishida, K.; Asayama, K.; Shimakawa, Y.; Manako, T.; Kubo, Y. NMR and NQR studies of superconductivity in heavily doped $\text{Tl}_2\text{Ba}_2\text{CuO}_{6+y}$ with a single CuO_2 plane. *Physica C* **1991**, *184*, 207–219.
22. Zheng, G.Q.; Kitaoka, Y.; Asayama, K.; Hamada, K.; Yamauchi, H.; Tanaka, S. NMR study of local hole distribution, spin fluctuation, and superconductivity in $\text{Tl}_2\text{Ba}_2\text{Ca}_2\text{Cu}_3\text{O}_{10}$. *Physica C* **1996**, *260*, 197–210.
23. Zheng, G.Q.; Sato, T.; Kitaoka, Y.; Fujita, M.; Yamada, K. Fermi-liquid ground state in the *n*-Type $\text{Pr}_{0.91}\text{LaCe}_{0.09}\text{CuO}_{4-y}$ copper-oxide superconductor. *Phys. Rev. Lett.* **2003**, *90*, 197005, doi:10.1103/PhysRevLett.90.197005.
24. Kotegawa, H.; Masaki, S.; Awai, Y.; Tou, H.; Mizuguchi, Y.; Takano, Y. Evidence for unconventional superconductivity in arsenic-free iron-based superconductor FeSe : A ^{77}Se -NMR study. *J. Phys. Soc. Jpn.* **2008**, *77*, 113703, doi:10.1143/JPSJ.77.113703.
25. Ishida, K.; Mukuda, H.; Kitaoka, Y.; Asayama, K.; Mao, Z.Q.; Mori, Y.; Maeno, Y. Spin-triplet superconductivity in Sr_2RuO_4 identified by ^{17}O Knight shift. *Nature* **1998**, *396*, 658–660.
26. Ishida, K.; Mukuda, H.; Kitaoka, Y.; Mao, Z.Q.; Fukazawa, H.; Maeno, Y. Ru NMR probe of the spin susceptibility in the superconducting state of Sr_2RuO_4 . *Phys. Rev. B* **2001**, *63*, 60507, doi:10.1103/PhysRevB.63.060507.
27. Mackenzie, A.P.; Maeno, Y. The superconductivity of Sr_2RuO_4 and the physics of spin-triplet pairing. *Rev. Mod. Phys.* **2003**, *25*, 657–712.
28. Duffy, J.A.; Hayden, S.M.; Maeno, Y.; Mao, Z.; Kulda, J.; McIntyre, G.J. Polarized-neutron scattering study of the Cooper-pair moment in Sr_2RuO_4 . *Phys. Rev. Lett.* **2000**, *85*, 5412–5415.
29. Deguchi, K.; Tanatar, M.A.; Mao, Z.Q.; Ishiguro, T.; Maeno, Y. Superconducting double transition and the upper critical field limit of Sr_2RuO_4 in parallel magnetic fields. *J. Phys. Soc. Jpn.* **2002**, *71*, 2839–2842.
30. Kittaka, S.; Nakamura, T.; Aono, Y.; Yonezawa, S.; Ishida, K.; Maeno, Y. Angular dependence of the upper critical field of Sr_2RuO_4 . *Phys. Rev. B* **2009**, *80*, 174514, doi:10.1103/PhysRevB.80.174514.
31. Machida, K.; Ichioka, M. Magnetic field dependence of low-temperature specific heat in Sr_2RuO_4 . *Phys. Rev. B* **2008**, *77*, 184515, doi:10.1103/PhysRevB.77.184515.
32. Zhang, J.; Lörcher, C.; Gu, Q.; Klemm, R.A. Is the anisotropy of the upper critical field of Sr_2RuO_4 consistent with a helical *p*-wave state? *J. Phys. Condens. Matter* **2014**, *26*, 252201, doi:10.1088/0953-8984/26/25/252201.
33. Annett, J.F.; Györfy, B.L.; Litak, G.; Wysokiński, K.I. Magnetic field induced rotation of the *d*-vector in Sr_2RuO_4 . *Physica C* **2007**, 460–462, 995–996.
34. Leggett, A.J. A theoretical description of the new phases of liquid ^3He . *Rev. Mod. Phys.* **1975**, *47*, 331–414.
35. Rozbicki, E.J.; Annett, J.F.; Souquet, J.-R.; Mackenzie, A.P. Spin-orbit coupling and *k*-dependent Zeeman splitting in strontium ruthenate. *J. Phys. Condens. Matter* **2011**, *23*, 94201, doi:10.1088/0953-8984/23/9/094201.

36. Suderow, H.; Crespo, V.; Guillamon, I.; Vieira, S.; Servant, F.; Lejay, P.; Brison, J.P.; Flouquet, J. A nodeless superconducting gap in Sr_2RuO_4 from tunneling spectroscopy. *New J. Phys.* **2009**, *11*, 93004, doi:10.1088/1367-2630/11/9/093004.
37. Berry, M.V. Quantal phase factors accompanying adiabatic changes. *Proc. R. Soc. Lond. A* **1984**, *392*, 45–57.
38. Griffiths, D.J. *Introduction to Quantum Mechanics*, 2nd ed.; Pearson: Upper Saddle River, NJ, USA, 2005.
39. Hattori, T.; Karube, K.; Ihara, Y.; Ishida, K.; Deguchi, K.; Sato, N.K.; Yamamura, T. Spin susceptibility in the superconducting state of the ferromagnetic superconductor UCoGe. *Phys. Rev. B* **2013**, *88*, 85127, doi:10.1103/PhysRevB.88.085127.
40. Aoki, D.; Flouquet, J. Ferromagnetism and superconductivity in uranium compounds. *J. Phys. Soc. Jpn.* **2012**, *81*, 11003, doi:10.1143/JPSJ.81.011003.
41. Gannon, W.J.; Halperin, W.P.; Rastovski, C.; Eskildsen, M.R.; Dai, P.C.; Stunault, A. Magnetism in the superconducting state of UPt_3 from polarized neutron diffraction. *Phys. Rev. B* **2012**, *86*, 104510, doi:10.1103/PhysRevB.86.104510.
42. Scharnberg, K.; Klemm, R.A. Upper critical field in p -wave superconductors with broken symmetry. *Phys. Rev. Lett.* **1985**, *54*, 2445–2448.
43. Hall, B.E.; Klemm, R.A. Microscopic model of the Knight shift in anisotropic and correlated metals. *J. Phys. Condens. Matter* **2016**, *28*, 03LT01, doi:10.1088/0953-8984/28/3/03LT01.
44. Haug, H.J.W.; Jauho, A.-P. *Quantum Kinetics in Transport and Optics of Semiconductors*; Springer: Berlin, Germany, 2008.
45. Klemm, R.A.; Clem, J.R. Lower critical field of an anisotropic Type-II superconductor. *Phys. Rev. B* **1980**, *21*, 1868–1875.
46. Klemm, R.A. Lower critical field of a superconductor with uniaxial anisotropy. *Phys. Rev. B* **1993**, *47*, 14630, doi:10.1103/PhysRevB.47.14630.
47. Anderson, P.W. Localized magnetic states in metals. *Phys. Rev.* **1961**, *124*, 41–53.
48. Lörscher, C.; Zhang, J.; Gu, Q.; Klemm, R.A. Anomalous angular dependence of the upper critical induction of orthorhombic ferromagnetic superconductors with completely broken p -wave symmetry. *Phys. Rev. B* **2013**, *88*, 24504, doi:10.1103/PhysRevB.88.024504.
49. Zhang, J.; Lörscher, C.; Gu, Q.; Klemm, R.A. First-order chiral to non-chiral transition in the angular dependence of the upper critical induction of the Scharnberg-Klemm p -wave pair state. *J. Phys. Condens. Matter* **2014**, *26*, 252202, doi:10.1088-8984/26/25/252202.
50. Rammer, J.; Smith, H. Quantum field-theoretical methods in transport theory of metals. *Rev. Mod. Phys.* **1986**, *58*, 323–359.
51. Drozdov, A.P.; Erements, M.I.; Troyan, I.A.; Ksenofontov, V.; Shylin, S.I. Conventional superconductivity at 203 K at high pressures in the sulfur hydride system. *Nature* **2015**, *525*, 73–77.
52. Werthamer, N.R.; Helfand, E.; Hohenberg, P.C. Temperature and purity dependence of the superconducting critical field H_{c2} . III. spin and spin-orbit effects. *Phys. Rev.* **1966**, *147*, 295–302.
53. Klemm, R.A.; Luther, A.; Beasley, M.R. Theory of the upper critical field in layered superconductors. *Phys. Rev. B* **1975**, *12*, 877–891.
54. Abrikosov, A.A.; Gor'kov, L.P.; Dzyaloshinskii, I.E. *Methods of Quantum Field Theory in Statistical Physics*; Prentice-Hall: Englewood Cliffs, NJ, USA, 1963.
55. Gor'kov, L.P. Microscopic derivation of the Ginzburg-Landau equations in the theory of superconductivity. *Sov. Phys. JETP* **1959**, *9*, 1364–1367.
56. Rickayzen, G. The theory of Bardeen, Cooper, and Schrieffer. In *Superconductivity*; Parks, R.D., Eds.; Marcel Dekker, Inc.: New York, NY, USA, 1969; pp. 51–115.
57. Klemm, R.A. Pristine and intercalated transition metal dichalcogenide superconductors. *Physica C* **2015**, *514*, 86–94.
58. Zhong, Y.; Wang, Y.; Han, S.; Lv, Y.-F.; Wang, W.-L.; Zhang, D.; Ding, H.; Zhang, Y.-M.; Wang, L.; He, K.; et al. Nodeless pairing in superconducting copper-oxide monolayer films on $\text{Bi}_2\text{Sr}_2\text{CaCu}_2\text{O}_{8+\delta}$. *Sci. Bull.* **2016**, *61*, 1239–1247.
59. Li, Q.; Tsay, Y.N.; Suenaga, M.; Klemm, R.A.; Gu, G.D.; Koshizuka, N. $\text{Bi}_2\text{Sr}_2\text{CaCu}_2\text{O}_{8+\delta}$ Bicrystal c -axis twist Josephson junctions: A new phase-sensitive test of order parameter symmetry. *Phys. Rev. Lett.* **1999**, *83*, 4160–4163.

60. Schaefer, H.F., III; Klemm, R.A., Harris, F.E. Atomic hyperfine structure. II. First-order wavefunctions for the ground states of B, C, N, O, and F. *Phys. Rev.* **1969**, *181*, 137–143.
61. Armstrong, L. Jr. *Theory of the Hyperfine Structure of Free Atoms*; Wiley Interscience: New York, NY, USA, 1971.



© 2018 by the author. Licensee MDPI, Basel, Switzerland. This article is an open access article distributed under the terms and conditions of the Creative Commons Attribution (CC BY) license (<http://creativecommons.org/licenses/by/4.0/>).